

SYNTHESIS AND MAGNETIC PROPERTIES OF Zn SPINEL CERAMICS

ŠTĚPÁN HUBER*, **, ZDENĚK SOFER*, #LADISLAV NÁDHERNÝ*, ONDŘEJ JANKOVSKÝ*,
PETR ŠIMEK*, DAVID SEDMIDUBSKÝ*, MIROSLAV MARYŠKO**

*Department of Inorganic Chemistry, Institute of Chemical Technology, Technická 5, 166 28 Prague 6, Czech Republic

**Institute of Physics of ASCR v.v.i., Cukrovarnická 10/112, 162 00 Prague 6, Czech Republic

#E-mail: ladislav.nadherny@vscht.cz

Submitted May 27, 2012; accepted June 16, 2013

Keywords: Zn spinel, Synthesis, Magnetic properties, Antiferromagnet, Bulk ZnO

We present the synthesis and characterization of $ZnTM_2O_4$ spinels (where $TM = Cr^{3+}, Mn^{3+}, Fe^{3+}$ and Co^{3+}), which are possible impurity phases in TM-doped ZnO that represent a large family of diluted magnetic semiconductors (DMS). The aim of our study was to find a uniform technique simplifying the whole synthesis of zinc spinels and their magnetic characterization. The synthesis was carried out by a conventional ceramic route with one calcination and two sintering steps. The structure of the prepared samples was proofed by X-ray diffraction analysis and magnetic properties were studied using SQUID magnetometer. Excluding the cobalt spinel, all spinels were single phase and showed antiferromagnetic behavior.

INTRODUCTION

Zn spinels belong to the group of magnetic oxides with broad use such as magnetic and switching devices [1-3]. Materials for spintronics represent another field of interest where spinels could play an important role. Diluted magnetic semiconductors (DMS) offer a great potential for development and construction of modern microelectronic and optoelectronic devices based on spin-transfer and data processing. These materials can exhibit ferromagnetic properties persisting well above room temperature. However, in case of ZnO based DMS there is still a controversy, whether its ferromagnetic behavior is really an intrinsic characteristic. As an alternative scenario, the unusual magnetic properties can be related to the phase separation in transition metal doped ZnO where the high Curie-temperature was predicted by Dietel [4].

Recently, the ferromagnetism was observed in zinc oxide doped by Mn and Co in the bulk material [5, 6] and also in the form of thin films [7, 8]. The origin of ferromagnetism in DMS zinc oxide can be however strongly affected by formation of other phases [9]. $ZnTM_2O_4$ (where the TM is Cr, Mn, Fe or Co) is one of the phases which can be formed due to the phase separation. In such spinel structure Zn ions prefer to occupy tetrahedral sites and TM is commonly distributed to octahedral sites [10]. Indeed, the formation of $ZnMn_2O_4$ and $ZnMnO_3$ phases was reported in ZnO doped by manganese [11]. Magnetic properties of Zn spinels have been studied in many works, among all, the system $Ni_xZn_{1-x}Mn_2O_4$ was studied by Bhandage and Keer [12];

magnetic susceptibility of $Zn_xMn_{3-x}O_4$ was published by Rosenberg and Nicolae [13]. Spin-lattice order in frustrated $ZnCr_2O_4$ was described by Ji et al. [14] and pressure-dependent properties of the same system were discussed by Jo and Park [15]. The magnetic structure of $ZnMn_2O_4$ was reported by Aiyama [16].

The aim of current research is to study the synthesis and the magnetic properties of Zn spinel phases. The knowledge of the magnetic characteristics of these phases is necessary for future interpretation of the respective properties of transition metal doped zinc oxide.

EXPERIMENTAL

Polycrystalline chromium, manganese, iron and cobalt spinels containing Zn in tetrahedral position were prepared by standard ceramic technology. The samples were synthesized from ZnO, Cr_2O_3 , $MnCO_3$, Fe_2O_3 and Co_2O_3 of 99.9 % or higher purity. Stoichiometric amounts of starting chemicals were mixed and processed by ceramic route involving one single calcination step and two sintering steps. The starting mixture was homogenized in an agate mortar and calcined in a platinum vessel at 800°C in the air for 48 hours. The calcined mixture was then re-homogenized in the mortar. The triturated fine powder was compacted into pellets on a hydraulic press (155 MPa) using stainless steel mould of one inch in diameter. The sintering was performed in the platinum vessel at 820°C in the air for 48 hours. Only the $ZnCo_2O_4$ spinel was treated in oxygen during the first sintering step. The sintered samples was

pulverized and milled in an agate planetary ball mill. The milling procedure was performed in methanol with a rotation speed of 600 s^{-1} for 30 minutes. The purity of the dried powder was probed by X-ray diffraction analysis. The powder was formed into 1 inch pellets by a hydraulic press (182 MPa) and subsequently sintered at 860°C in oxygen for 48 hours (1000°C and 122 hours for ZnCo_2O_4).

The powder X-ray diffraction patterns were recorded by X'Pert PRO powder diffractometer (PANanalytical, The Netherlands) with parafocusing Bragg-Brentano geometry using $\text{Cu-K}\alpha$ radiation ($\lambda = 1.5418 \times 10^{-1} \text{ nm}$) and ultrafast detector (X'Celerator). The X-ray diffraction was measured in the range of $5 - 80^\circ 2\theta$ with a step size of 0.02° . The unit-cell parameters and ion site occupancies were refined by Rietveld method using FullProf Suite software [17]. Magnetic properties were characterized by SQUID magnetometer (MPMS-5, Quantum Design). Magnetization and magnetic susceptibility were measured in the temperature range of $4 - 300 \text{ K}$ and the magnetic field up to 5 T. The magnetic moment as a function of temperature was measured in a magnetic field of 0.1 T.

RESULTS AND DISCUSSION

Structural properties

The phase purity of the samples was confirmed by comparing experimental X-ray diffraction patterns (Figure 1) and reference cards from JCPDS/PDF database. While the Co sample contained unreacted ZnO; Cr, Mn and Fe based samples exhibit single phase spinel composition. The unit-cell parameters evaluation (Table I.) revealed that all samples had cubic ($\text{Fd}\bar{3}\text{m}$) symmetry, except for ZnMn_2O_4 which exhibited tetragonal symmetry ($\text{I4}_1/\text{amd}$) as a result of strong Jahn-Teller effect of Mn^{3+} occupying the octahedral site.

The Rietveld refinement suggested traces of Fe^{3+} in tetrahedral position in ZnFe_2O_4 sample which was presumably compensated by Zn^{2+} in octahedral site. If this was not the case, the occupation of tetrahedral position by Fe^{3+} would result in a precipitation of ZnO in the sample. Nonetheless, neither the occurrence of Zn^{2+}

in octahedral site nor any ZnO impurities were detected. Both ZnMn_2O_4 and ZnCr_2O_4 were found apparently free of impurities. On the other hand, the quantitative phase fraction analysis using Rietveld method performed on ZnCo_2O_4 revealed 80 % of the spinel phase and 20 % of ZnO (P6₃mc). This indicates the spinel exhibited a mixed valence state of $\text{Co}^{3+}/\text{Co}^{2+}$, where Co^{3+} and Co^{2+} ions occupy both the octahedral and tetrahedral positions, respectively. The cobalt valences in the respective positions were also confirmed by the bond valence sum analysis applied on the bond lengths from structure refinement results. Consequently, the Zn^{2+} was displaced from the tetrahedral positions by Co^{2+} substitution forming $\text{Zn}_{1-x}\text{Co}_x\text{Co}_2\text{O}_4$ and $x \text{ ZnO}$ phase. The refined tetrahedral site occupancy – 0.5 Zn^{2+} , 0.5 Co^{2+} – was in a good agreement with the obtained phase ratio. The observed phase separation is apparently due to a relatively low oxygen activity during the synthesis which imposes the formation of Co^{2+} . To avoid this effect and to stabilize the pure spinel with Co^{3+} occupying exclusively the octahedral site, we suggest that either a higher oxygen pressure or much lower temperature during the synthesis is necessary.

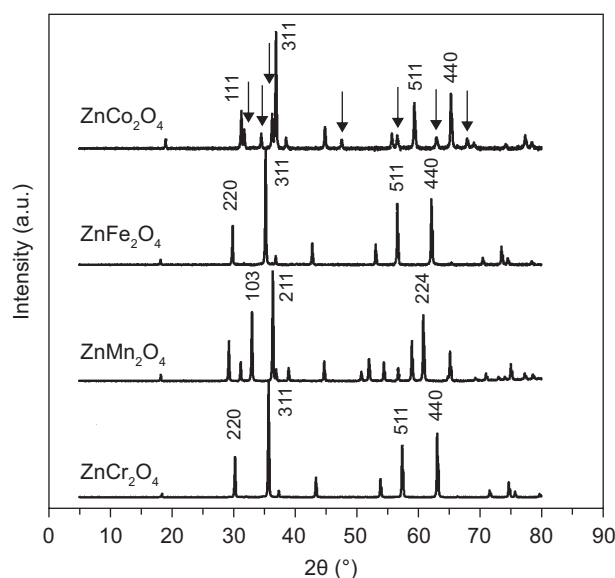


Figure 1. X-ray powder diffraction patterns of the synthesized spinels. Zinc oxide besides ZnCo_2O_4 labeled by arrows.

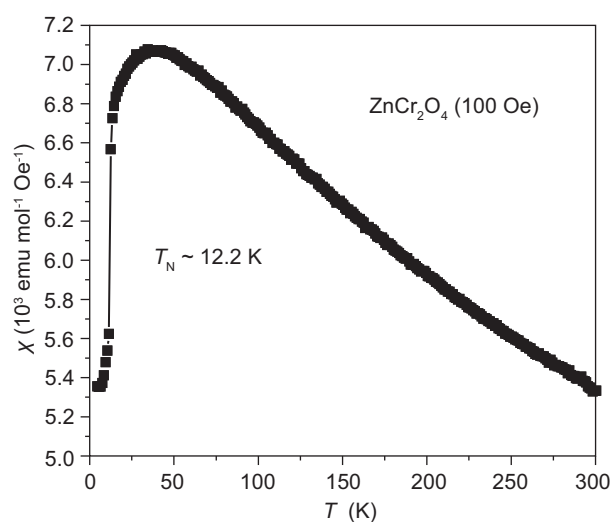
Table 1. Structural and magnetic parameters of the prepared spinel obtained by XRD analysis (including Rietveld refinement) and SQUID magnetometry, respectively.

Chemical formula	Space group	Lattice parameter		Magnetic behavior	Magnetic moment m (μ_B/TM^{3+})	Néel temperature T_N (K)
		a (10^{-1} nm)	c (10^{-1} nm)			
ZnCr_2O_4	$\text{Fd}\bar{3}\text{m}$	8.324 7(3)	–	antiferromagnetic	3.3	12
ZnMn_2O_4	$\text{I4}_1/\text{amd}$	5.720 0(2)	9.222 4(4)	antiferromagnetic	–	–
ZnFe_2O_4	$\text{Fd}\bar{3}\text{m}$	8.441 6(4)	–	antiferromagnetic	–	15
ZnCo_2O_4	$\text{Fd}\bar{3}\text{m}$	8.085 3(6)	–	antiferromagnetic	2.5	–
ZnO (in ZnCo_2O_4)	$\text{P6}_3\text{mc}$	3.253 2(4)	5.201 0(8)	diamagnetic	–	–

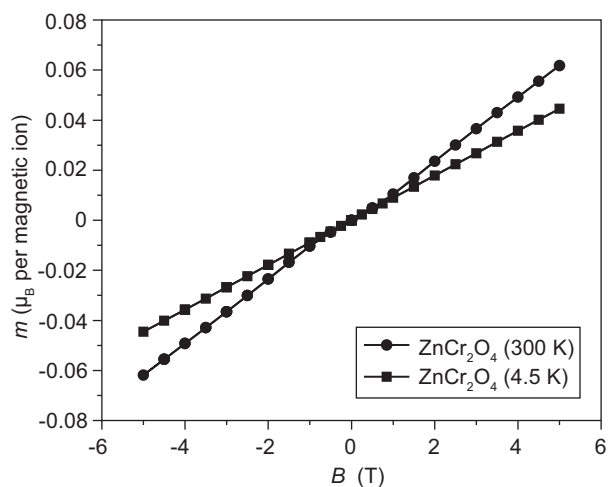
Magnetic properties

Provided the excessive ZnO in the cobalt spinel is diamagnetic, this sample was also suitable for magnetic characterization by SQUID magnetometer. If, moreover, the small amount of Co was dissolved in wurtzite structure of ZnO, its concentration in $\text{Zn}_{1-x}\text{Co}_x\text{O}$ would be still too low to affect noticeably the analysis of spin moment in the paramagnetic region.

Magnetization curves of ZnCr_2O_4 at 300 K and 4.5 K (Figure 2b) showed a non-hysteretic behavior. The susceptibility vs. temperature measurement (Figure 2a) exhibited a Curie-Weiss paramagnetic behavior in the high temperature range ($3.3 \mu_B/\text{Cr}$), which is coherent with presence of Cr^{3+} in B sites. An antiferromagnetic behavior below the Néel temperature, $T_N \sim 40$ K (short-range, the susceptibility starts to decrease) and T_N at 12 K (long-range order), was observed. Same susceptibility



a) magnetic susceptibility

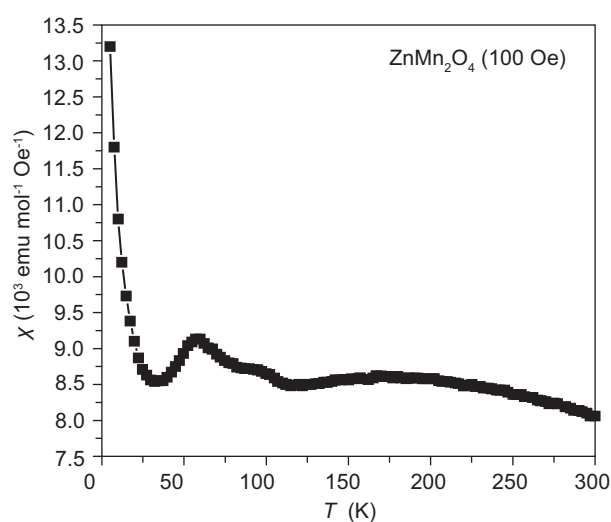


b) magnetization curves

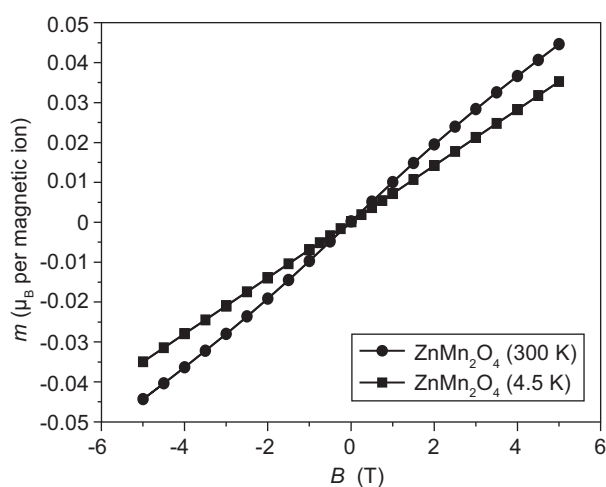
Figure 2. Magnetic susceptibility (a) and magnetization curves (b) of ZnCr_2O_4 .

reflecting both the short and long-range orders Sianou et al. reported the similar long-range Néel temperature (T_N) of ZnCr_2O_4 approximately at 12.5 K [18]. A similar T_N was observed by Glazkov et al. on a single crystal sample [19]. Chen et al. suggested the antiferromagnetic transition can even disappear when particles reach the critical size [20].

Although ZnMn_2O_4 should in general behave as an antiferromagnet, it was not possible to determine the T_N unambiguously. Unfortunately, the available literature data are also rather vague. While Aiyama [16] attributed the Néel temperature to a broad maximum located approximately at 210 K corresponding to exceedingly strong exchange interactions, Åsbrink et al. [21] identified $T_N \sim 21.5$ K as a temperature of an abrupt increase of magnetic susceptibility which is not a behavior typical for an antiferromagnet. As seen from Figure 3a two maxima (at 180 K and 60 K) and a sharp



a) magnetic susceptibility



b) magnetization curves

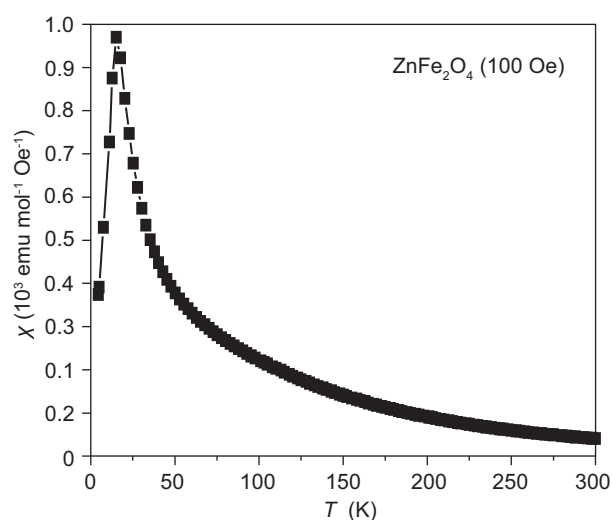
Figure 3. Magnetic susceptibility (a) and magnetization curves (b) of ZnMn_2O_4 .

rise at low temperatures (starting at ~ 25 K) can be observed on our temperature dependence of susceptibility. A very similar magnetic susceptibility behavior of the ZnMn-spinel was observed by Shoemaker [22]. In the high temperature limit the magnetic susceptibility obeys the Curie-Weiss law with highly negative Curie temperature ($\theta_C \sim -910$ K); however it apparently starts to diverge from the ideal paramagnetic behavior below 250 K. This can be attributed to short-range antiferromagnetic interactions, whereas the long-range antiferromagnetic order is presumably established below 60 K [23]. The maximum observed at 60 K is consistent with that reported by Shoemaker [22], but it has not been confirmed in other studies [16, 23]. The low temperature rise is likely associated with magnetic impurities, not detected by XDR. Eventually, a small part of Zn in tetrahedral position can be replaced by Mn^{2+} as demonstrated in [22, 23]. This substitution leads to a significant increase

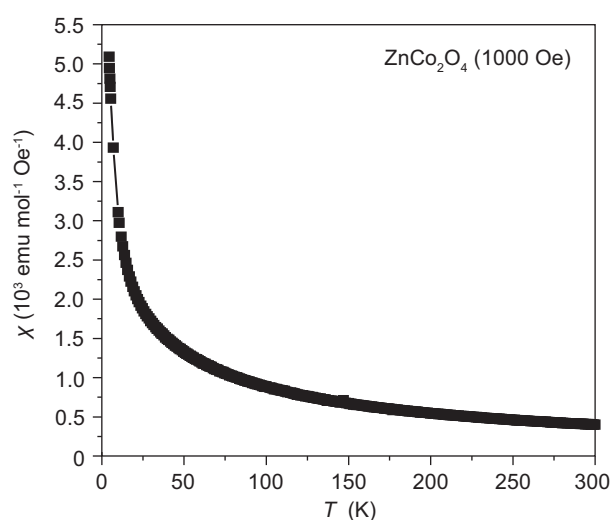
of $\chi(T)$ due to the short-range ferrimagnetic order with an onset temperature depending on the substitution rate.

The data measured on Fe-based spinel are in agreement with already published values [24]. The magnetic susceptibility curves recorded for $ZnFe_2O_4$ sample on heating after zero field cooling (ZFC) and field cooled (FC) have one local maximum corresponding to the value of T_N approximately at 15 K (Figure 4a). Above this temperature, the susceptibility corroborated by the magnetization curve at 300 K (Figure 4b) and excluding a simple estimation of Curie constant exhibited a paramagnetic-like behavior. However, the temperature dependence of inverse susceptibility was not linear. The magnetization curve at 4.5 K (Figure 4b) showed no hysteresis and $ZnFe_2O_4$ can be thus intrinsically regarded as a low temperature antiferromagnet.

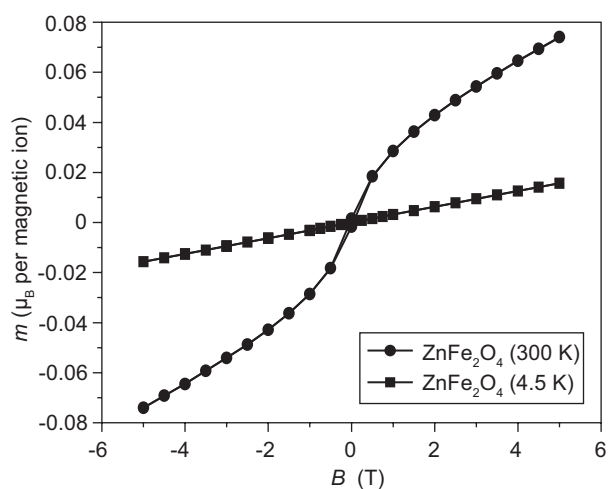
Although any antiferromagnetic transition was not identified from the measured magnetic susceptibility



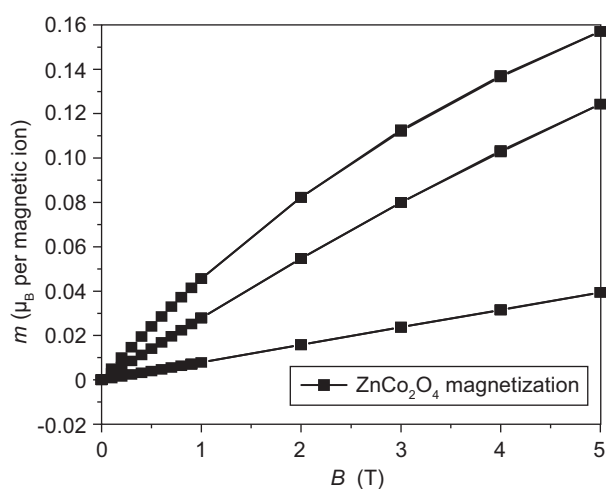
a) magnetic susceptibility



a) magnetic susceptibility



b) magnetization curves



b) magnetization curves

Figure 4. Magnetic susceptibility (a) and magnetization curves (b) of $ZnFe_2O_4$.

Figure 5. Magnetic susceptibility (a) and magnetization curves (b) of $ZnCo_2O_4$.

(Figure 5a), the negative Weiss constant corroborated the antiferromagnetic behavior ($\theta_C \sim -75$ K) of the ZnCo_2O_4 sample. The magnetization curves (Figure 5b) also showed no hysteresis in the measured temperature range. The average spin moment $\sim 2.5 \mu_B/\text{Co}$ (assuming Co stoichiometry of 2.5) evaluated from the temperature dependence of the paramagnetic susceptibility suggested Co^{2+} in tetrahedral position bearing the spin $3 \mu_B$ and a mixed low-intermediate or low-high spin state of Co^{3+} in octahedral position [25].

CONCLUSION

All the Cr, Mn and Fe based Zn spinels can be successfully synthesized by standard ceramic procedure with final heat treatment performed in pure oxygen atmosphere.

The Rietveld analysis of XRD data confirmed a direct spinel ZnTM_2O_4 structure with TM^{3+} in octahedral position for $\text{TM} = \text{Cr}$ and Mn , and no traces of reactants. In case of ZnFe_2O_4 spinel was indicated a possible partial exchange between Fe^{3+} and Zn^{2+} in octahedral and tetrahedral sites. In contrast, the O_2 oxidation potential during the final heat treatment was not sufficient to stabilize pure Co^{3+} . Instead, in ZnCo_2O_4 a phase separation into ZnO and $\text{Zn}_{0.5}\text{Co}_{2.5}\text{O}_4$, exhibiting a mixed $\text{Co}^{2+}/\text{Co}^{3+}$ valence state (0.5 Co^{2+} in tetrahedral position) was observed. Higher oxygen pressure or lower heating temperature would be thus necessary to synthesize the pure spinel.

Although the interpretation of the measured magnetic properties was complicated due to the mentioned phase separation in the case of Co, and a possible formation of magnetic inhomogeneities in the case of Fe and Mn, all spinel phases under the study were found to be intrinsic antiferromagnets at low temperature.

Acknowledgements

This work was supported by the Czech Science Foundation (grant N° 13-17538S), Ministry of Education of the Czech Republic (research projects N° MSM6046137302 and project for specific university research 20/2013) and the bilateral Czech-French project Barrande (7AMB12FR019).

REFERENCES

1. Chantrell, R. W., Ogrady, K.: *Appl. Magn.* 253, 113 (1994).
2. Nakamura, T., Tsutaoka, T., Hatakeyama, K.: *J. Magn. Mater.* 138, 319 (1994).
3. Tsutaoka, T., Ueshima, M., Tokunaga, T., Nakamura, T., Hatakeyama, K.: *J. Appl. Phys.* 78, 3983 (1995).
4. Dietl, T., Ohno, H., Matsukura, F., Cibert, J., Ferrand, D.: *Science*. 287, 1019 (2000).
5. Sharma, P., Gupta, A., Owens, F. J., Inoue, A., Rao, K. V.: *J. Magn. Mater.* 282, 115 (2004).
6. Jayakumar, O. D., Gopalakrishnan, I. K., Kulshreshtha, S. K.: *J. Mater. Chem.* 15, 3514 (2005).
7. Venkatesan, M., Fitzgerald, C. B., Lunney, J. G., Coey, J. M. D.: *Phys. Rev. Lett.* 93, 177206-1 (2004).
8. Bacaksiz, E., Aksu, S., Basol, B. M., Altunbas, M., Parlak, M., Yamnaz, E.: *Thin Solid Films*. 516, 7899 (2008).
9. Liu, C., Yun, F., Morkoc, H.: *J. Mater. Sci. - Mater. Electron.* 16, 555 (2005).
10. Henderson, C. M. B., Charnock, J. M., Plant, D. A.: *J. Phys.: Condens. Matter*. 19, (2007).
11. Blasco, J., Bartolome, F., Garcia, L. M., Garcia, J.: *J. Mater. Chem.* 16, 2282 (2006).
12. Bhandage, G. T., Keer, H. V.: *J. Phys. C: Solid State Phys.* 11, L219 (1978).
13. Rosenberg, M., Nicolae, I.: *Phys. Status Solidi*. 5, K127 (1964).
14. Ji, S., Lee, S. H., Broholm, C., Koo, T. Y., Ratcliff, W., Cheong, S. W., Zschack, P.: *Phys. Rev. Lett.* 103, 37201-1 (2009).
15. Jo, Y., Park, J. G., Kim, H. C., Ratcliff, W., Cheong, S. W.: *Phys. Rev. B: Condens. Matter*. 72, 184421-1 (2005).
16. Aiyama, Y.: *J. Phys. Soc. Jpn.* 21, 1684 (1966).
17. Rodríguez-Carvajal, J.: *Physica B*. 192, 55 (1993).
18. Sianou, A. K., Stergioudis, G. A., Efthimiadis, K. G., Kalogirou, O., Tsoukalas, I. A.: *J. Alloys Compd.* 392, 310 (2005).
19. Glazkov, V. N., Farutin, A. M., Tsurkan, V., von Nidda, H. A. K., Loidl, A.: *Phys. Rev. B: Condens. Matter*. 79, 1 (2009).
20. Chen, X. H., Zhang, H. T., Wang, C. H., Luo, X. G., Li, P. H.: *Appl. Phys. Lett.* 81, 4419 (2002).
21. Asbrink, S., Waskowska, A., Gerward, L., Olsen, J. S., Talik, E.: *Phys. Rev. B: Condens. Matter*. 60, 12651 (1999).
22. Shoemaker, D. P., Rodriguez, E. E., Seshadri, R., Abumohor, I. S., Proffen, T.: *Phys. Rev. B: Condens. Matter*. 80, 144422-1 (2009).
23. Troyanchuk, I. O., Szymczak, H., Kasper, N. V.: *Phys. Status Solidi A*. 157, 159 (1996).
24. Chinnasamy, C. N., Narayanasamy, A., Ponpandian, N., Chattopadhyay, K.: *Mater. Sci. Eng., A*. 304, 983 (2001).
25. Krezhov, K., Konstantinov, P.: *J. Phys.: Condens. Matter*. 5, 9287 (1993).